Understanding Pulsar Wind Nebulae: recent progress and open questions

Elena Amato [⋆]

INAF-Osservatorio Astrofisico di Arcetri, Largo E. Fermi, 5, I-50125, Firenze, Italy

Abstract I present a short review of our current understanding of Pulsar Wind Nebulae (PWNe). I will try to highlight the recent progress made towards solving some long standing puzzles concerning the physics of these objects. The main focus will be on the problems related to the dissipation of the pulsar wind energy and to the acceleration of the relativistic particles that produce the non-thermal nebular emission. The kind of observations that will possibly provide, in the near future, important information concerning some of the open problems will also be discussed, together with some possible lines of development of future theoretical work.

Key words: acceleration of particles – MHD – neutrinos – shock waves – stars: winds, outflows – supernova remnants

1 INTRODUCTION

Pulsar Wind Nebulae, sometimes referred to as *plerions*, are the calorimeters that collect the rotation energy lost by fast-spinning magnetized neutron stars, that may or may not manifest themselves as pulsars. As the electromagnetic torques acting on such a star cause it to spin-down, most of the rotational energy it loses does not result in direct magnetospheric emission but it is rather converted into the acceleration of a highly relativistic magnetized wind.

If this wind is efficiently confined by the surrounding Supernova Remnant (SNR), then a considerable fraction of the energy lost by the star can be revealed as non-thermal emission of the magnetized, relativistically hot plasma forming a nebula around the star. This nebula is what we define as a PWN. The spin-down luminosity of the star that goes into feeding the PWN is recovered after integration of the nebular emission over a wide range of frequencies, usually extending from the radio to the X-ray and even γ-ray band. The prototype of this class of objects, the Crab Nebula, has been observed in a range of frequencies spanning more than 15 decades, and together with three other members of its class, it has even been detected with confidence at TeV photon energies (e.g. Guetta & Amato 2003).

Presently about 30 PWNe have been identified. The rate of new discoveries has greatly increased during the last few years, mainly due to the progress of X-ray astronomy, that has become the preferential channel for finding new members of this class and is promising to largely

⋆ E-mail: amato@arcetri.astro.it

increase the number of known plerions in the near future. Despite the recent progress, however, the best studied plerion so far and the one for which most of the current ideas concerning the physics of these nebulae have been worked out is still the Crab Nebula.

In fact, it is not clear whether this object can be considered as really prototypical, in that it is especially young and powered by a pulsar with an exceptionally high spin-down luminosity. Moreover, its surrounding supernova remnant (SNR) is expanding at an unusually slow rate, hence providing particularly efficient confinement of the relativistic fluid enclosed. These two facts, on the one hand, make it especially bright in all frequency bands and hence more suitable for detailed studies than any other member of the class, on the other hand, they make one question whether its physics is really representative of the entire class.

In the following we shall discuss some of the puzzles that the attempts at modeling the dynamics and emission properties of the Crab Nebula have brought to light and the recent progress that has been made towards their solution.

2 GENERAL THEORY OF PULSAR WIND NEBULAE

The schematic picture of a plerion is shown in Fig. 1, where one can see the cold, highly relativistic wind emanating from the star being slowed down at a termination shock. In the outer region a bubble of relativistically hot magnetized fluid is created and that is where the non-thermal nebular emission originates from. The confining supernova remnant partly penetrates the bubble as a consequence of Rayleigh-Taylor instabilities: some of the material ejected in the supernova explosion is found within the synchrotron nebula in the form of elongated structures or *filaments*.
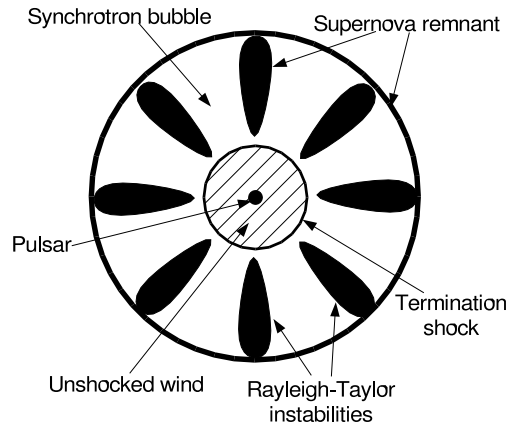
Fig. 1 Schematic picture of a plerion: see text for description.

A combination of theory and observations leads to a number of general conclusions about the properties of the wind that emanates from the pulsar. First of all, the wind must be mainly made of electron-positron pairs due to the copious pair-production that takes place in the pulsar magnetosphere, with possibly a minor fraction of ions, most probably either protons or highly ionized iron nuclei. In spite of being a minority by number, the ions could still be energetically dominant in the wind, due to their much larger mass when compared to the pairs: the possible consequences of this fact will be discussed later on.

Before the termination shock the wind Lorentz factor is estimated to be in the range $10^4 < \Gamma < 10^7$ and a toroidal magnetic field is frozen in the flow. At the termination shock the

outflow is slowed down so that it can match the condition of subrelativistic expansion at the outer boundary of the nebula. The acceleration of particles producing the power-law spectrum that it is then observed as the source of the non-thermal emission of the nebula is thought to be produced as part of the dissipation process that takes place at the shock, turning the bulk kinetic energy of the wind into heat.

In the case of the Crab Nebula, the pulsar wind termination shock is spatially resolved and identified with the position of the so called optical *wisps*. These are variable features in the optical surface brightness distribution of the nebula that are located at the outer boundary of an underluminous central region surrounding the pulsar, whose identification with the propagation zone of the unshocked relativistic wind is straightforward.

The first attempt at modeling the spatial distribution of the fluid in the Crab Nebula was made by Rees & Gunn (1974), who looked for a steady state 1-dimensional hydrodynamical (HD) solution in spherical symmetry. This very crude model was already able to correctly predict the wind termination shock position R_s. This turns out to be given, in terms of the nebular radius (R_N) and expansion velocity (V_N), as $R_s \approx R_N \sqrt{V_N/3c}$. Inserting into this relation the values of R_N and V_N appropriate for the Crab Nebula, one obtains an estimate of R_s that is fully consistent with the position of the wisps.

A refinement of the hydro model mentioned above is the 1D steady state ideal magneto-hydrodynamical (MHD) model by Kennel & Coroniti (1984), who included the magnetic field in the dynamics (Kennel & Coroniti 1984a) and also attempted at fitting the nebular emission (Kennel & Coroniti 1984b). They managed to reproduce the surface brightness profile of the Crab Nebula at optical and X-ray frequencies assuming a cold MHD wind propagating from the vicinities of the pulsar out to the termination shock at a speed corresponding to a bulk Lorentz factor $\Gamma \sim 10^6$. Two puzzles arose however from their modeling. First of all no radio emitting particles could be fit in the treatment: these have an average Lorentz factor that is $\Gamma_r \approx 10^4$ and are much more abundant by number than the higher energy (optical and X-ray emitting) particles, for which the Lorentz factor is estimated to be $\Gamma_{OX} \approx 3 \times 10^6$. Hence, including them among the population of particles continuously accelerated at the shock would require the upstream wind Lorentz factor to be $\Gamma \sim \Gamma_r \sim 10^{-2}\Gamma_{OX}$ and at the same time the particle injection rate would have to be $\dot{N} \sim 10^{40} \text{s}^{-1}$, i.e. a factor 10^2 larger than that estimated based on the optical/X-ray emitting particles, $\dot{N}_{OX} \sim 10^{38} \text{s}^{-1}$.

In addition to the mystery related to the origin of the radio-emitting particles, another puzzle became clear from the dynamical modeling of the nebula, the so called σ-*paradox*. Let us define σ as the ratio between Poynting flux and kinetic energy flux in the unshocked pulsar wind: $\sigma \equiv B^2/4\pi\rho\Gamma c^2$. This parameter is expected to be much larger than unity in the vicinity of the pulsar, since strong electromagnetic fields are at the origin of the pulsar behavior. In particular, at the light cylinder distance, current pulsar theories predict, for the Crab Nebula, $\sigma(R_{LC}) \sim 10^4 \gg 1$. However, the best fit value of σ in the solution by Kennel & Coroniti was $\sigma \sim 3 \times 10^{-3}$ just upstream of the shock. Such a low value of σ was confirmed by both the 1D self-similar treatment by Emmering & Chevalier (1987) and the 2D steady-state MHD solution by Begelman & Li (1992). On the other hand, attempts at reproducing the Crab Nebula emission within the framework of high σ models were unsuccessful: in order to explain the optical and X-ray emission a diffusion coefficient four orders of magnitude larger than the Bohm diffusion coefficient is required (Amato et al. 2000). This is too large a value to be compatible with an ordered magnetic field such as it is deduced for the Crab Nebula from polarization maps.

A number of solutions have been proposed during the years to the σ paradox. The first attempts (Coroniti 1990; Michel 1994) involved magnetic reconnection in a striped pulsar wind. This is the flow structure expected for an oblique rotator, i.e. a configuration in which the toroidal magnetic field has opposite orientations in the two hemispheres around the pulsar spin

equator, and its polarity changes in the equatorial plane on a length-scale $\lambda = R_{\mathrm{LC}}$. Other proposals calling for non-ideal MHD effects involved either large amplitude waves (Melatos & Melrose 1996), in which case σ would be reduced in the process of wave-mode conversion triggered by parametric instabilities, or nozzle type effects (Chiueh et al. 1998).

A partial solution to the paradox was recently presented within the framework of ideal MHD by Contopoulos & Kazanas 2002. They showed, given the field structure in the overdense magnetosphere of an aligned rotator found by Contopoulos et al. (1999), that the system acts like a linear accelerator. As long as their inertia is negligible, the particles move outward with the drift velocity of the field lines and their Lorentz factor Γ increases linearly with distance. This implies that σ decreases linearly with distance (see definition). If this behavior extends out to the distance where $\sigma \sim 1$ (further out the plasma inertia starts dominating and both Γ and σ keep constant with distance) then a terminal wind Lorentz factor $\Gamma \sim 10^{6.5}$, exactly the best fit value in the model by Kennel & Coroniti, is obtained.

Of course, even $\sigma = 1$ would not be suitable for the Crab Nebula and further reduction is required. Moreover, the linear acceleration mechanism discussed above cannot actually extend out to the point where $\sigma \sim 1$, but only to the fast magnetosonic point, where $\sigma \sim \Gamma^2$ (see, for example, Kirk & Skjaeraasen 2003).

Recent progress has also been made on the study of another mechanism that we mentioned as a possible explanation for the reduction of the wind magnetization, i.e. relativistic magnetic reconnection. After this process seemed to be too slow to provide the decrease of σ between R_{LC} and R_{s} needed in the case of the Crab Nebula (Lyubarsky & Kirk 2001), recent reexaminations (Lyutikov & Uzdensky 2003; Lyutikov 2003; Kirk & Skjaeraasen 2003) suggest it as viable again. Interestingly enough, according to the analysis by Kirk & Skjaeraasen, the particle injection rate required so that magnetic reconnection could account alone for the terminal magnetization of the Crab pulsar wind is $\dot{N} \geq 10^{40}\ \mathrm{s}^{-1} \sim \dot{N}_{\mathrm{R}}$, i.e. the estimated injection rate of radio emitting particles.

3 PARTICLE ACCELERATION IN PULSAR WIND NEBULAE

Apart from the problem of understanding whether the radio emitting particles are accelerated in the same way as the X-ray emitting ones, a more general puzzle related to the origin of suprathermal particles in PWNe concerns the mechanism that is at work to provide the acceleration. Although, as I mentioned, at least in the case of the particles with Lorentz factors above 10^7 (i.e. those responsible for the nebular X-ray synchrotron emission), there is a general consensus that acceleration takes place at the termination shock, the process that is at work to provide it is not well understood. This is due to the peculiar structure of this shock, that makes both the mechanisms usually invoked to explain particle acceleration in astrophysical objects non viable in this context. The most common acceleration process at astrophysical shocks is diffusive shock acceleration (Fermi I process). This mechanism, however, only works at quasi-parallel shocks, i.e. shocks whose geometry is such that the magnetic field is aligned to the shock normal within an angle $\theta_{\mathbf{B} \cdot \mathbf{n}} \ll 1/\Gamma$, with Γ the Lorentz factor of the fluid upstream of the shock as measured in the shock reference frame. It is clear that in the case of an outflow with a Lorentz factor in the range that we mentioned ($10^4 < \Gamma < 10^7$), even if the magnetic field were tangled, and not (as is thought to be the case in plerions) exactly perpendicular to the shock normal, nevertheless the sections of the shock that could satisfy this condition would occupy only a small part of the total area. An alternative mechanism that is believed to operate in the quasi-perpendicular geometry is the shock drift acceleration process (Begelman & Kirk 1990). However, in order to work, this latter mechanism requires that the Larmor radius of the particles to be accelerated be much larger than the thickness of the shock. Neither this condition can be satisfied at the pulsar wind termination shock in plerions, where the particles

to be accelerated are the same forming the shock and hence determining its thickness. The conclusion is that some non-standard acceleration mechanism is required to be at work.

The most successful proposed answer so far is based on the process of resonant cyclotron absorption (RCA) in a ion-doped plasma. The basic idea behind this mechanism (see Fig. 2) is as follows. All species $(e^+ - e^- - p)$ initially drift towards the shock front. The enhanced magnetic field at the shock causes the particles to start gyrating. At the leading edge of the shock, the distribution of the particles in transverse (with respect to the magnetic field direction) momentum-space is well described as a cold ring, a configuration that is known to be cyclotron unstable. The gyration is accompanied by relativistic cyclotron emission, with a spectrum extending, for each species, from its basic Larmor frequency in the background magnetic field up to very high harmonic multiples of this. The gyration frequencies of the pairs are much larger than those of the ions if the drift velocity before the shock was the same for all species. The pairs interact through absorption and emission of cyclotron waves and thermalize on a very short time-scale compared to the interaction time-scale of the ions. The instability in the pairs does not affect the ions because these cannot interact efficiently with the waves generated by the pairs since these waves are too high frequency for them. On the time-scales on which the instability in the ions takes place, the pairs already form a thermal background plasma, at a temperature that is of order of the kinetic energy per particle upstream of the shock.

In such condition the collective radiation emitted by the ions as they become unstable can grow at all frequencies up to the pairs' average gyration frequency. Moreover, the growth rate is expected to be almost independent on harmonic number, based on the linear theory of this instability for a spatially uniform, perfectly cold ion plasma immersed in a thermal pair plasma (see Fig. 3). If there is enough power in the waves emitted by the ions at the gyration frequency of the pairs (i.e. corresponding to the nth harmonic with n the mass ratio between the ions and the pairs), the $e^+ - e^-$ can resonantly absorb these waves. As the absorption process proceeds the pairs can absorb lower and lower harmonic multiples of the ion gyration frequency and get accelerated up to a maximum energy that is of order of the initial kinetic energy of the ions.
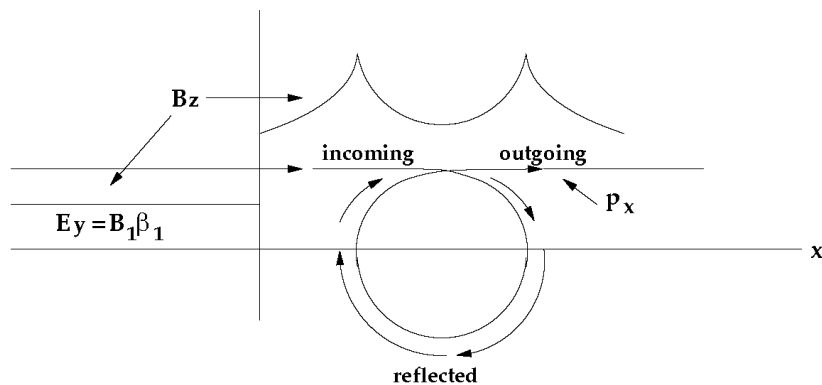
Fig. 2 Schematic representation of the leading edge of a transverse relativistic shock. The plasma drifts towards the shock front from the left. The enhancement of the magnetic field at the shock causes the particles to stop drifting and start gyrating. If the ions are energetically dominant, a further enhancement of the magnetic field intensity is produced at the reflection points of their orbits.
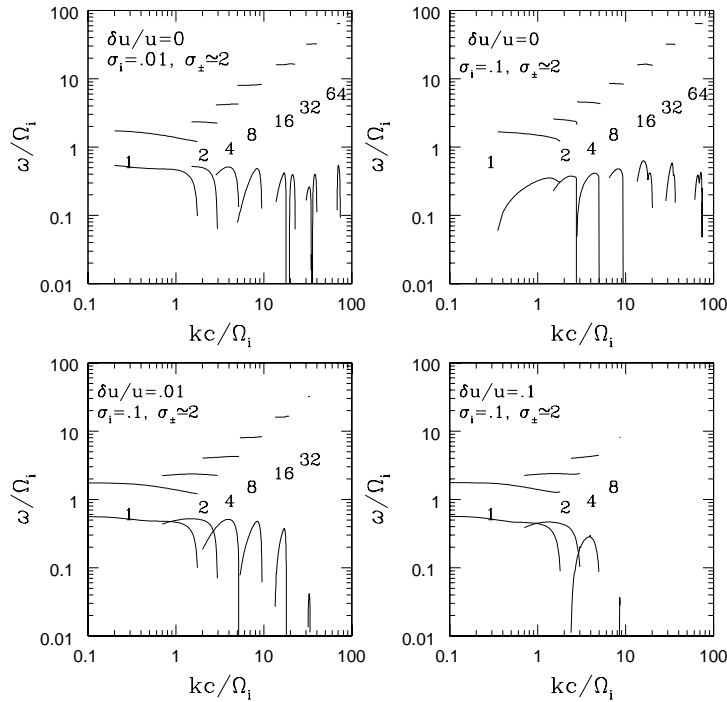
Fig. 3 Linear growth rate of the ion cyclotron instability in a spatially uniform background thermal pair plasma. In each panel the upper curves correspond to the real part of the dispersion relation, while the lower curves are the growth rates. The different panels show how the solution of the dispersion relation depends on the ratio between the magnetic and kinetic energy of the plasma (σ) and on the thermal spread $\delta u/u$ of the initial ions' distribution. From comparison of the two panels on top, we notice that the growth rates are larger for less magnetized plasmas. The two panels below show how the spectrum is cutoff at harmonics higher than $\omega = n_{\rm crit}\,\Omega_{\rm ci}$ with $n_{\rm crit} \sim u/\delta u$ ($\Omega_{\rm ci}$ is the relativistic ion Larmor frequency).

Previous numerical investigations of the problem, through Particle In Cell (PIC) simulations, showed that this mechanism could actually guarantee an efficient energy transfer from the ions to the positrons when the ions are the energetically dominant species (Hoshino & Arons 1991; Hoshino et al. 1992). In those early investigations, however, due to computational limitations, the mass-ratio between the ions and the pairs was bound to be $m_{\rm i}/m_{\pm} = 20$ at most (to be compared with the realistic value of $m_{\rm i}/m_{\pm} \approx 2000$ at least).

Since the entire acceleration process crucially depends on whether there is initially enough power at the harmonic $n = m_{\rm i}/m_{\pm}$, we performed a new investigation (Amato & Arons 2003), using the PIC code XOOPIC (Verbonocouer et al. 1995) and adopting mass-ratios up to $m_{\rm i}/m_{\pm} = 100$. We found that, with increasing mass-ratio, not only the acceleration of positrons is still possible, although its efficiency is somewhat reduced and the resulting particle spectrum somewhat steeper, but we also found, for the first time, evidence of electron acceleration, as one can see from Fig. 4.

The differences between the present simulations and the old ones, and in particular the fact that we find acceleration of electrons as well as positrons, are easily understood in terms of differences in the polarization of the waves between the different simulation plasmas. We know

from linear theory that the ion waves that can grow in the plasma are in general elliptically polarized and tend to have a polarization closer to linear the closer to neutral (equal number of positive and negative charges) the background pair plasma is. Since the overall $e^+ - e^- - p$ plasma is neutral, the polarization of the waves will be closer to linear the fewer the ions are by number. But a fundamental condition for the acceleration process to take place is that the ions be energetically dominant. In order for this condition to be satisfied one has to include an increasingly smaller fraction of ions in the simulation as the mass-ratio is increased. Having the ions energetically dominant with a mass ratio of only 20 forces one to include so many ions in the simulation that the waves they emit result to be very close to circularly polarized and as a result the positrons can absorb them very efficiently (more effectively than if they were linearly polarized), while the electrons cannot. The validity of this interpretation is supported by the results shown in Fig. 5, where we compare two simulations in which the same fraction of energy is put into ions but with different combinations of mass and number ratios.

The overall efficiency of the process and the spectra of accelerated particles it produces turn out to depend on the fraction of energy that the ions carry and on the thermal spread of the initial ions' distribution. When the results are extrapolated to the realistic mass ratio, only a very small fraction of ions is required in order to obtain acceleration of the pairs. A more stringent (but still possible to satisfy) requirement is that the thermal spread in their initial energy distribution be such that $\delta u/u < 5 \times 10^{-4}$. However, this new study of the RCA process leads us to conclude that this model still stands as the most promising for explaining particle acceleration in PWNe. In the following section possible observational tests of this acceleration model will be discussed.
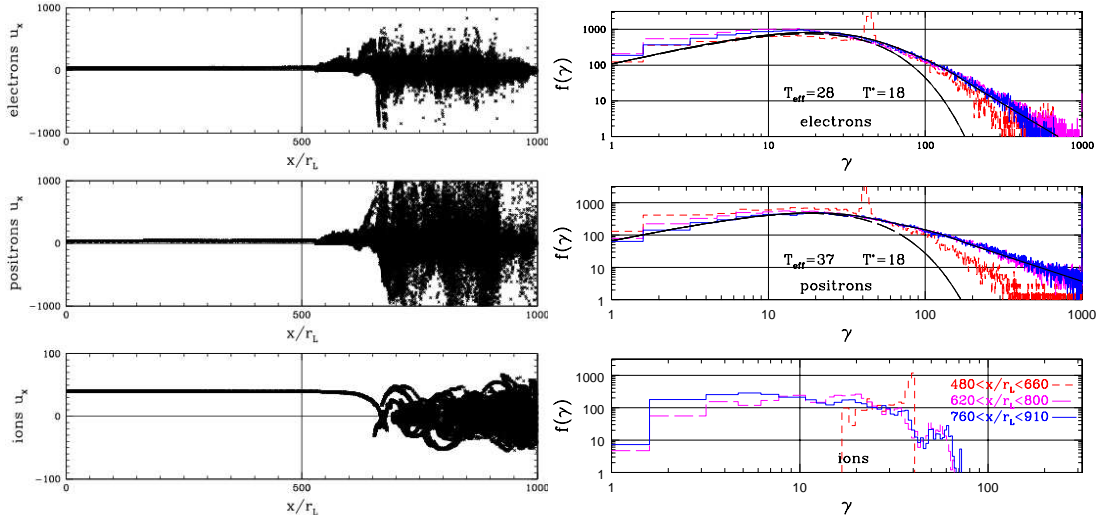
Fig. 4 Results of a simulation with $m_i/m_\pm = 100$. Left panel: distribution of the particles in $(x - u_x)$ space; it is apparent that the ions are still cold when the pair velocities are already thermally spread; the shock front is at $x \approx 600$. Right panel: three snapshots of the particle distribution function taken from slices of the simulation box at different distances behind the shock; the thick solid curve is a maxwellian at the temperature the pairs should have in the absence of energy exchange with the ions, while the thick dashed curve is a maxwellian plus power-law tail that allows to fit the real distribution.
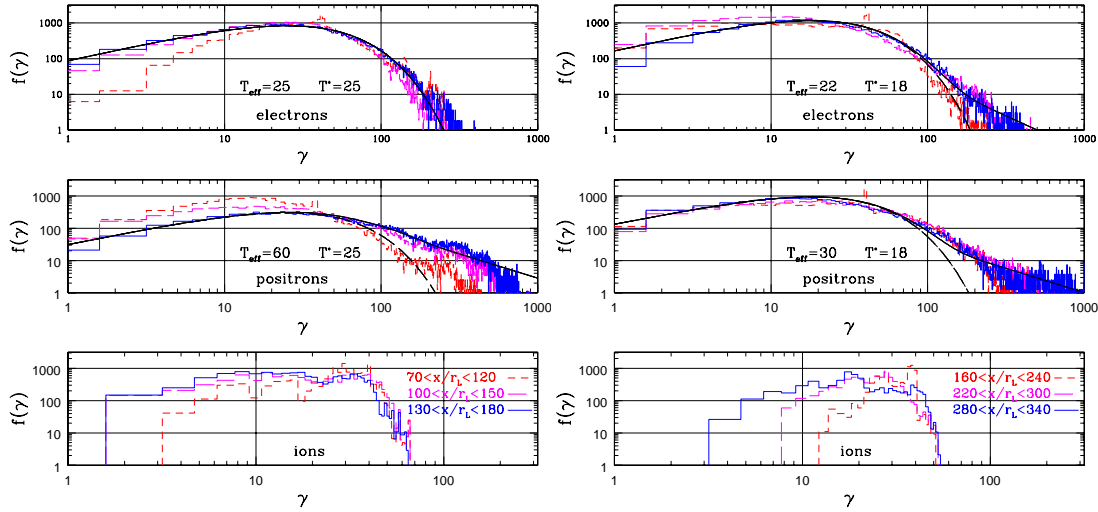
Fig. 5 Comparison between the particle distributions resulting from two simulations with the same fraction of energy into ions but with differently polarized waves. The notation is the same as for the right panel in Fig. 4. The panel on the left and that on the right refer to simulations which employ a mass ratio between the ions and the pairs $m_i/m_\pm = 20$ and $m_i/m_\pm = 40$ respectively: so the simulation shown on the left contained twice as many ions as that on the right. In the case on the left no electron acceleration is found: the electron distribution can be well fitted with a relativistic Maxwellian, while the suprathermal tail of positrons, at the end of the acceleration process, shows an extremely flat spectrum. In the panel on the right, signs of electron acceleration start to be observable while the efficiency at accelerating positrons is reduced.

4 OBSERVATIONAL TESTS OF THE RCA MODEL FOR PARTICLE ACCELERATION

4.1 Variability in γ-rays

The interpretation of the particle acceleration in plerions as due to the RCA process in a ion-doped plasma has some interesting observational consequences. One of the reasons why this model has been considered successful is that it provides a natural interpretation for two main observational features of the Crab Nebula, namely the wisps' (see section 2) separation and variability and the maximum energy at which particles are accelerated. The wisps are interpreted as due to the magnetic field compression at the turning points of the first few ion gyration orbits. Their average spacing and variability on time-scales of order months can be interpreted in terms of the gyration of the ions (Gallant et al. 1994, Spitkovsky & Arons 1999) assuming a Lorentz factor of the wind that is exactly of the order of what is estimated based on dynamical modeling of the nebula (Kennel & Coroniti 1984a, 1984b): $\Gamma \approx 4 \times 10^6$. For this same value of the wind Lorentz factor, one finds that the maximum particle energy has a value very close to what implied by the observed cutoff of the nebular synchrotron spectrum (de Jager et al. 1996). In fact, for a maximum energy of the pairs equal to the initial ions' energy $E_{max} \approx 4 \times 10^{15}$eV, gyration in the downstream magnetic field $B_2 \approx 10^{-4}$G leads to

the estimate $\epsilon_{\text{sync}} \approx 20 \, \text{MeV}$ as the maximum energy of synchrotron emitted photons, fully compatible with the observed value.

The fact that the nebular synchrotron emission spectrum cuts off at this energy makes it especially interesting to observe the Crab Nebula in the energy range 50–100 MeV. In particular one should look for time-variability of the emission in this energy range. Since, based on the model discussed above, the shock structure is unsteady, we also expect the particle acceleration process to vary. At particle energies such that the synchrotron loss-time is much larger than the acceleration time-scale, the variations average out. At higher energies, however, the acceleration time-scale becomes comparable to the synchrotron loss-time and one expects to see variability of the emission on time-scales of order months. A rough estimate of the variability to be expected may be obtained by simply comparing the time-scales for acceleration and losses. The result is that variability in excess of 10% of the synchrotron emission in the 50–100 MeV photon energy range should be observed on time-scales of order few months. Upcoming γ-ray telescopes such as GLAST should be able to detect it.

4.2 Signatures of protons

The most peculiar feature of the acceleration mechanism proposed, however, is the requirement that protons (more generally ions) be present in the pulsar wind and carry most of the energy. If this is the case, it is worth speculating on how one could detect them directly. The primary mechanism of energy losses through which the highly relativistic protons required could reveal themselves is pion-production. Both charged and neutral pions can be produced and then decay into electrons and neutrinos (the former), or very high energy (multi-TeV) γ-rays (the latter).

In PWNe there are two basic targets with which the protons can interact to produce pions, namely the nebular radiation field and the thermal matter of the supernova ejecta, which, as we mentioned, partly penetrates the nebula itself. Interaction with the latter is much more effective and pion-production through nuclear collisions turns out to be competitive with the other types of energy losses that limit the protons' life-time, namely adiabatic and escape losses. The efficiency of the pion production process depends on two main unknown quantities, i.e. the protons' energy, which is related to the wind Lorentz factor upstream of the shock and determines the importance of escape losses, and the effective density of the target for collisions in the nebula. The latter is especially difficult to determine or even constrain because as we mentioned the distribution of the thermal matter in the nebula is highly non-uniform, the density of the concentrations is not known, nor is their filling factor in the nebular volume. Moreover, we do not know the structure of the magnetic field near and within the Rayleigh-Taylor filaments, nor its intensity. In principle the magnetic field could prevent the relativistic protons from ever getting into the filaments, as well as trap them for very long times once they get in. We parametrized the unknowns related to the collision probability introducing a parameter μ relating the effective target density to the average target density in the nebula, computed as though the entire mass of the ejecta were uniformly distributed in the PWN volume: $n_{\text{t}} = \mu \, \bar{n}$.

We evaluated (Amato et al. 2003) the consequences of pion-production losses by the relativistic protons at different stages of the evolution of a Crab-like plerion. In Fig. 6 we show the contribution coming from pion-decay to the radiation spectrum of a plerion as a function of its age and of the wind Lorentz factor, assuming that the effective target density is that equivalent to 1 $M_\odot$ of material uniformly distributed in the nebula ($\mu = 1$), and that the energy of the wind is equally shared between protons, pairs and magnetic field. It is apparent from the figure that although secondary pairs are unlikely to contribute significantly to the nebular spectrum, it is in principle possible to detect the γ-rays contributed by π^0-decay even in plerions that are hundreds of years old.
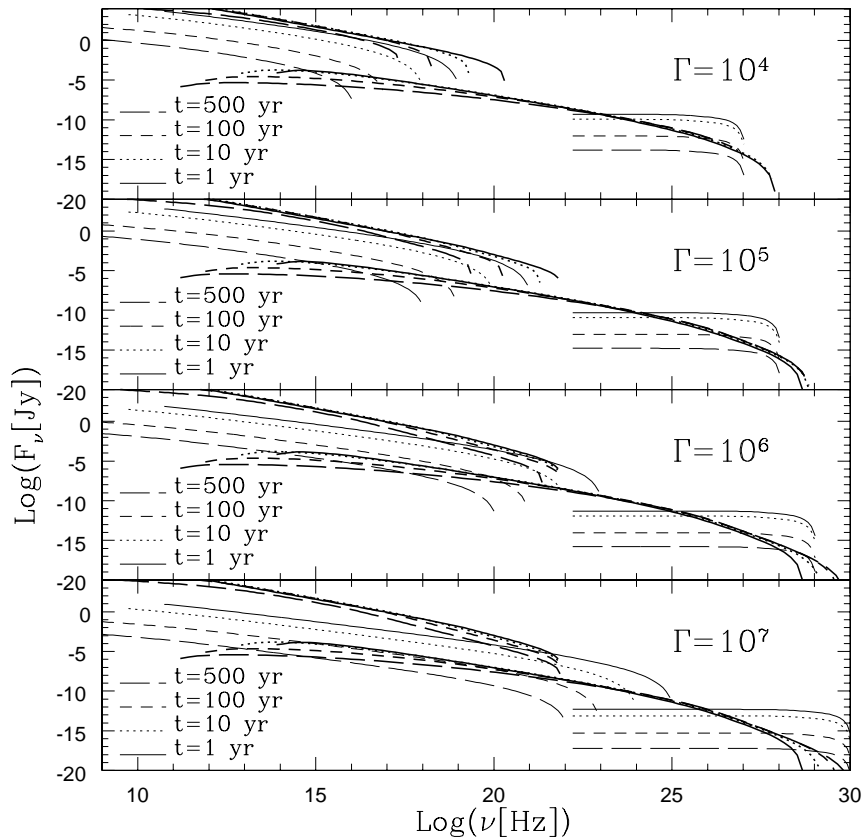
Fig. 6 The contribution of pion-decay products to the radiation spectrum of a young plerion. The different panels correspond to different values of the wind Lorentz factor. The different line-styles correspond to different ages as specified in the panels. The thick curves represent the radiation spectrum (due to synchrotron at lower energies and to Inverse Compton scattering at higher energies) produced by the primary pairs, those directly accelerated at the shock. The thin curves refer, at low frequencies, to the synchrotron emission of the secondary pairs from charged pion decay, and, at high energies, to γ-rays directly produced by π^0-decay.

When one applies this calculation to the case of the Crab Nebula, for which data, or at least upper limits, are available also at the highest energies, the result is extremely interesting. In Fig. 7 we show the high energy part of the Crab Nebula spectrum. For the case when protons carry 60 % of the total energy of the wind: this is the best fit value for reproducing the wisps within the framework of the RCA model (Spitkovsky & Arons 1999), the curves representing the contribution of π^0-decay are found to exceed the data and upper limits for some combinations of values of μ and Γ.

This fact allowed us to constrain the combined parameter space for these three unknowns, as shown in the left panel of Fig. 8. These results are better understood after noticing that $\mu = 8$ corresponds to an effective target density equivalent to having the entire mass contained in the ejecta (Fesen et al. 1997) uniformly distributed in the nebula, while $\mu = 20$ is the maximum possible value of this parameter based on the constraint that bremsstrahlung radiation does not
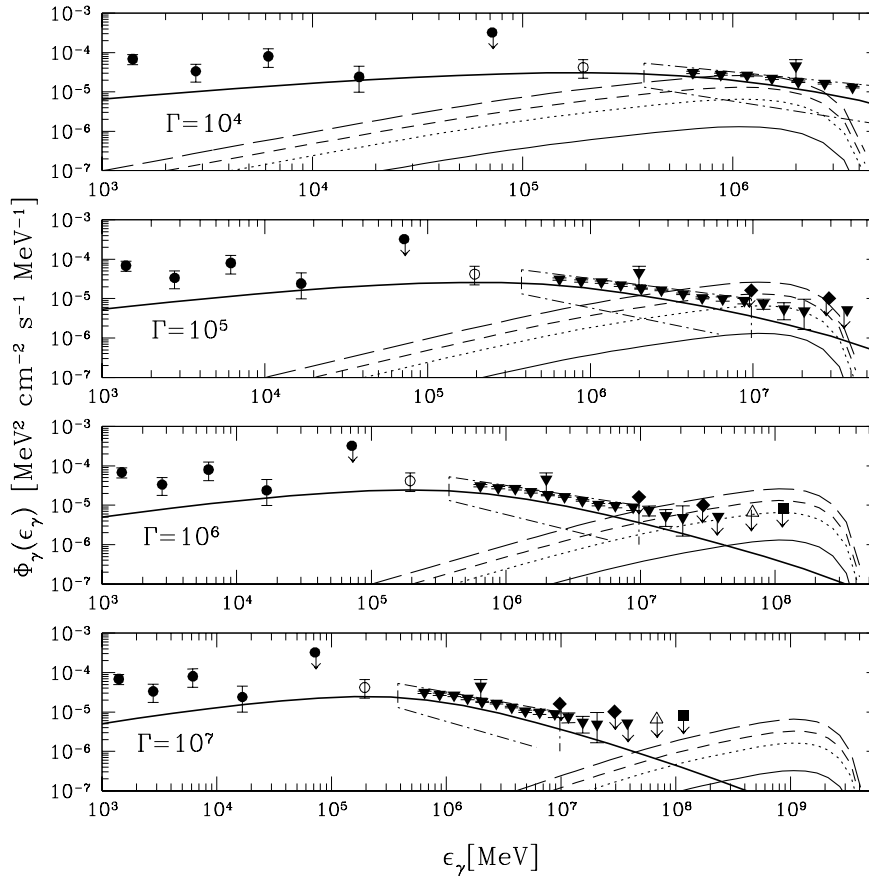
Fig. 7 Consequences of pion-production on the spectrum of the Crab Nebula. The high energy spectrum of the nebula is shown. The points represent the observed data and upper limits (de Jager et al. 1996; Aharonian et al. 2000). The thick curve represents the ICS (Inverse Compton Scattering) spectrum of the nebula that provides a good interpretation of the available data. The thin curves represent the γ-rays contributed by π^0-decay for different values of the parameter μ: $\mu = 1$ is the solid line, $\mu = 5$ dotted, $\mu = 10$ short-dashed, $\mu = 20$ long-dashed. All curves are computed assuming that 60 % of the wind total luminosity is in protons.

exceed the X-ray data (Atoyan & Aharonian 1996). It is interesting to notice that for $\mu = 10$ or larger the possibility that 60 % of the pulsar wind luminosity might be in protons with a Lorentz factor $\Gamma = 4 \times 10^6$ would already be excluded by the data. Upcoming TeV γ-ray experiments are expected to further constrain the allowed parameter space for high values of the wind Lorentz factor.

Of course the most direct signature of protons in the wind would be detection of high energy neutrinos. While TeV γ-rays may result from ICS (this is in fact the standard interpretation of the TeV spectrum of the Crab Nebula) as well as from hadronic processes, neutrinos can only result from the latter. We computed the maximum flux of neutrinos from the Crab Nebula allowed by the TeV data (right panel of Fig. 8) showing that this is above the background of next-generation neutrino telescopes for most of the plausible values of Γ.
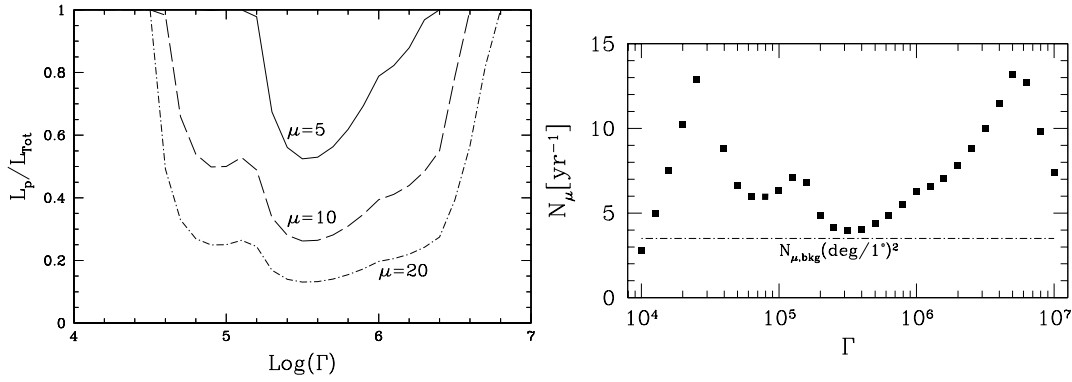
Fig. 8 Left panel: the allowed regions of the parameter space $L_p/L_{tot} - \Gamma$ are determined as a function of μ; the allowed combinations of the parameters are those in the area below each curve ($\mu = 5 \rightarrow$ solid, $\mu = 10 \rightarrow$ dashed, $\mu = 20 \rightarrow$ dot-dashed). Right panel: the maximum number of muons per year that would be produced by neutrinos coming from the Crab Nebula in a km^2 detector; the dot-dashed line represents the background counts for a detector with 1deg^2 angular resolution.

5 SUMMARY AND CONCLUSIONS

I discussed the recent theoretical progress made towards understanding the physics of PWNe, focusing on two major aspects: the σ paradox and the mechanism responsible for particle acceleration. Concerning the latter, I mainly discussed the developments of our recent reanalysis (Amato & Arons, in prep.) of the RCA process in a ion-doped plasma as the source of particle acceleration at the pulsar wind termination shock, also mentioning the results of a preliminary attempt at quantitatively evaluating the observational consequences of having most of the wind energy carried by ions. The possibility of obtaining a final answer to this question seems to be at hand with the upcoming experiments in the γ-ray band and the next generation of neutrino telescopes, although a number of uncertainties enter the model predictions. An effort to quantify some of these uncertainties is currently under way.

As a final point, I would like to mention the importance that numerical simulations via the relativistic MHD codes that have recently become available (e.g. Del Zanna et al. 2003 and references therein) are likely to assume in the progress of this field. Detailed comparison between increasingly high quality data and numerical experiments is in fact promising to provide us with answers concerning a number of unknowns, ranging from the details of the PWN evolution to the consequences of its interaction with the surroundings and even to a reliable estimate of parameters intrinsic of the pulsar wind.

References

Aharonian F.A. et al., 2000, ApJ, 539, 317

Amato E., Salvati M., Bandiera R., Pacini F., Woltjer L., 2000, A&A, 359, 1107

Amato E., Guetta D., Blasi P., 2003, A&A, 402, 827

Amato E., Arons J., in prep.

Atoyan A.M., Aharonian F.A., 1996, MNRAS, 278, 525

Begelman M.C., Kirk J.G., 1990, ApJ, 353, 66

Begelman M.C., Li Z.-Y., 1992, ApJ, 397, 187

Chiueh T., Li Z.Y., Begelman M.C., 1998, ApJ, 505, 835

Contopoulos J., Kazanas D., Fendt C., 1999, ApJ, 511, 351

Contopoulos J., Kazanas D., 2002, ApJ, 566, 336

Coroniti F. V., 1990, ApJ, 349, 538

Del Zanna L., Bucciantini N., Londrillo P., 2003, A&A, 400, 397

Emmering R.T., Chevalier R.A., 1987, ApJ, 321, 334

Fesen R.A., Shull J.M., Hurford A.P., 1997, AJ, 113, 354

Gallant Y. A., Arons J., 1994, ApJ, 435, 230

Guetta D., Amato E., 2003, Astroparticle Physics, 19, 403

Hoshino M., Arons J., 1991, Phys. Fluids B, 3, 818

Hoshino M., Arons J., Gallant Y., Langdon A.B., 1992, ApJ, 390, 454

de Jager O.C. et al., 1996, ApJ, 457, 253

Kennel C.F., Coroniti F.V., 1984a, ApJ, 283, 694

Kennel C.F., Coroniti F.V., 1984b, ApJ, 283, 710

Kirk J. G., Skjaeraasen O., 2003, ApJ, 591, 366

Lyubarsky Y., Kirk J. G., 2001, ApJ, 547, 437

Lyutikov M., Uzdensky D., 2003, ApJ, 589, 893

Lyutikov M., 2003, astro-ph/0210353

Melatos A., Melrose D. B., 1996, MNRAS, 279, 1168

Michel F.C., 1994, ApJ, 431, 397

Rees M.J., Gunn J.E., 1974, MNRAS, 167, 1

Spitkovsky A., Arons J., 1999, AAS, 195, 3304

Verbonocoeur J.P., Langdon A.B., Gladd N.T., 1995, Computer Physics Communications, 87, 199